In Vivo Measurement of the Human Lumbar Spine Using Magnetic Resonance Imaging to Ultrasound Registration

Terry K. Koo, PhD,[a] Robert L. Crews, BS,[a] and Wingchi E. Kwok, PhD[b]

Abstract

Objective: This study aimed to refine a magnetic resonance imaging (MRI)-ultrasound registration (ie, alignment) technique to make noninvasive, nonionizing, 3-dimensional measurement of the lumbar segmental motion in vivo.
Methods: Five healthy participants participated in this validation study. We scanned the lumbar region of each participant 5 times using an ultrasound probe while he or she kept a prone lying posture on a plinth. Participant-specific models of L1-L5 were constructed from magnetic resonance (MR) images and aligned with the 3-dimensional ultrasound dataset of each scan using 4 variants of MRI-ultrasound registration approach (simplified intensity-based registration [1] with and [2] without including the transverse processes and their surrounding soft tissues [denoted as TP complex]; and hierarchical intensity-based registration [3] with and [4] without including the TP complex). The robustness and precision of these registration approaches were compared.
Results: Although all registration approaches converged to a similar solution, excluding the TP complex improved the percentage of successful registration from 92% to 100%. There was no significant difference in the precision among the 4 MRI-ultrasound registration variants. For the simplified intensity-based registration without including the TP complex, average precision at each degree of freedom was 1.33° (flexion-extension), 2.48° (lateral bending), 1.32° (axial rotation), 2.15 mm (left/right), 1.08 mm (anterior-posterior), and 1.16 (superior-inferior), respectively.
Conclusion: Given that using simplified intensity-based MRI-ultrasound registration can substantially streamline the registration process and excluding the TP complex would improve the robustness of the registration, we conclude that this combination is the method of choice for in vivo human applications. (J Manipulative Physiol Ther 2019;42:343-352)
Key Indexing Terms: *Ultrasonography; Magnetic Resonance Imaging; Lumbar Vertebrae*

Introduction

In vivo measurement of 3-dimensional (3D) segmental lumbar kinematics is important to our understanding of the normal and pathologic biomechanics of the lumbar spine. Although it is generally agreed that people move differently in the presence of low back pain,[1,2] in vivo human data showing the effects of low back pathology on intervertebral kinematics are scarce. Degenerative disc disease itself causes segmental hypomobility at the affected lumbar motion segment and hypermobility at the adjacent motion segments.[3] This observation implies that the pain generator may alter lumbar segmental motion pattern in a specific manner, and therefore, in vivo lumbar segmental motion could be a potential quantitative measure to help locate the anatomical location of the source of low back pain. In chiropractic medicine, such information may be used to evaluate the effects of spinal manipulative therapy on improving segmental hypomobility, which has been proposed as one of the mechanisms of action of spinal manipulative therapy on low back pain.[4] It can also facilitate objective assessment of spinal deformities (eg, scoliosis).[5]

However, because of the anatomical complexity, extensive degrees of freedom, and voluminous and heterogeneous soft tissue content of the human lumbar spine, in vivo lumbar segmental motion measurements continue to be technically challenging. Even though numerous methods—including skin marker tracking,[6] implanted marker tracking,[7] bi-plane radiography,[8,9] dual fluoroscopy,[10] computed tomography,[11] and dynamic magnetic resonance imaging (MRI)[12] — have been proposed to make 3D spinal measurements, these approaches are highly invasive, prone to substantial errors,

[a] Foot Levelers Biomechanics Research Laboratory, New York Chiropractic College, Seneca, Falls, NY.
[b] Department of Imaging Sciences, University of Rochester, University of Rochester Center for Advanced Brain Imaging & Neurophysiology, Rochester, NY.
Corresponding author: Terry K. Koo, PhD, Foot Levelers Biomechanics Research Laboratory, New York Chiropractic College, 2360 State Route 89, Seneca Falls, NY 13148.
Tel.: +1 315 568 3158. (e-mail: *tkoo@nycc.edu*).
Paper submitted January 10, 2019; in revised form March 8, 2019; accepted March 30, 2019.
0161-4754

https://doi.org/10.1016/j.jmpt.2019.03.008

involve repetitive ionizing radiation, or require the participants to be tested at nonfunctional or non-weight-bearing states. We recently developed a noninvasive, nonionizing imaging technique, namely MRI-ultrasound registration (ie, alignment), aiming to address these technical challenges, and performed a series of in vitro and in situ experiments on a human dry bone phantom (T12-L5) and porcine cadaver (L2-L6) to validate the technique by comparing with ground true solutions determined from implanted fiducial markers.[13] The basic premise of the MRI-ultrasound registration is to apply geometric transformations to participant-specific MRI-reconstructed vertebral models so that they align with the 3D freehand ultrasound dataset of the corresponding lumbar vertebrae that were acquired during actual pose measurements. This way, the 3D pose of each vertebra can be estimated. Although our results showed that the MRI-ultrasound registration is accurate (bias at the sub-degree and sub-millimeter levels) and reliable (precision better than 1.3° in rotation and 1.2 mm in translation),[13,14] it is not known whether the registration technique can be directly extended to live human participants. This uncertainty exists because the previous validation experiments cannot completely mimic either the geometry or the acoustic environment of the live human lumbar spine. Specifically, the human dry bone phantom that was used in our previous study was submerged in a water bath, which produced much better ultrasound images for registration use. Although the porcine cadaver is a more realistic model to evaluate the MRI-ultrasound registration technique, its dimension and geometry and the acoustic properties of the surrounding soft tissues could still be quite different from the live human participants.

Given that human participants are the target group of any clinical applications, it is imperative to further evaluate the MRI-ultrasound technique using live human participants before it can be applied clinically to make in vivo 3D measurement of the human lumbar spine. Therefore, the objective of this study was to refine the MRI-ultrasound registration technique to make it more suitable for live human participant application. Specifically, we compared the robustness and precision of 4 variants of the MRI-ultrasound registration technique on a cohort of human participants and made recommendation based on these results. We hypothesized that there was no difference in precision and robustness among the 4 variants of the MRI-ultrasound registration technique.

Materials and Methods

Participant Population

A convenient sample of 7 healthy participants was recruited from the student and staff population of New York Chiropractic College. Exclusion criteria included previous surgery of the spine, a history of low back pain in the past 24 months, nonzero visual analog pain rating or Oswestry disability Index at the time of testing, abnormal spinal curvature as determined by Adam's forward bend test, current pregnancy or possibility of pregnancy, poor ultrasound image at the lumbar region, broken or irritated skin or scar tissue at the lumbar region, a history of allergy to ultrasound gel, and presence of contraindications for MRI scan. Participants gave informed consent for the investigation according to the procedure approved by the institutional review board of New York Chiropractic College and the University of Rochester. Ultrasound image quality was assessed by checking whether the left and right superior and inferior articular processes and the spinous processes of each lumbar vertebra could be confidently identified from the ultrasound images. Two participants were excluded from the study because of poor ultrasound image quality. The mean (standard deviation) age and body mass index of the tested participants (3 male and 2 female) were 26.4 (4.2) years and 21.5 (2.1) kg/m^2, respectively.

MR Imaging and Processing

For each participant, 3D spoiled gradient echo sequence was used to acquire MR images of the lumbar spine in the sagittal plane. All scans were acquired by a Siemens 3-Tesla MAGNETOM Prisma system (Siemens Healthineers, Erlangen, Germany) using a standard spine coil. The imaging parameters were repetition time = 15 ms, echo time = 3.0 ms, flip angle = 15°, field of view = 256 × 256 mm^2, matrix size = 256 × 256, number of slices = 144, image resolution = 1.0 × 1.0 × 1.0 mm^3, receive bandwidth = 450 Hz/pixel, and scan time = 9:14 minutes. Respiratory gating was not used, and the participant was instructed to breathe quietly during scanning.

3D Doctor software (Able Software Corp, Lexington, Massachusetts) was used to segment and construct participant-specific vertebral models of L1 to L5. Segmentation was achieved by manually tracing vertebral boundaries from MR images using an active pen on the touchscreen display of a laptop computer in the tablet mode. Compared with the conventional approach of tracing the vertebral boundaries using a computer mouse, this approach was deemed to result in more precise and faster segmentation. The MRI voxels that corresponded to the posterior bone surface of each vertebra were extracted from each vertebral model using a modified forward ray tracing method.[14] The extracted MRI voxels were then used as an input to the MRI-ultrasound registration.

Four landmarks (anterior, posterior, left, and right points on the superior endplate) were also digitized from each vertebral model to define a vertebral anatomical coordinate system.[8] Specifically, the origin was defined as the mean coordinates of the 4 landmarks. A unit vector from the posterior to the anterior point of the superior endplate was defined as the y-axis. The z-axis was defined as the cross product of a unit vector from the left to the right point of the superior endplate and the y-axis, and the x-axis was the

cross product of the y- and z-axes. Hence, x-, y-, and z-axes of each vertebra pointed to the right, anterior, and superior, respectively.

Ultrasound Imaging and Processing

A freehand 3D ultrasound system described in our previous work[5] was used to acquire a 3D ultrasound dataset of the whole lumbar spine. Its main components included an ultrasound scanner (Ultramark 400c, ATL Ultrasound Inc, Bothell, Washington) with a 3.5- to 5-MHz curvilinear transducer to image the lumbar spine and an optoelectronic measurement system (Northern Digital Inc, Waterloo, Canada) to track the 3D poses of the transducer. The system was first calibrated by an actuator-assisted calibration approach,[15] and the point reconstruction accuracy of the calibrated system was determined to be 0.11 mm. To facilitate the acquisition of high-quality axial ultrasound images throughout the lumbar region, a marking protocol was proposed. First, a trained research assistant palpated and marked the spinous processes of L1 to L5. A smooth line was then traced along the spinous processes, which defined a scanning trajectory for a 3.5- to 5-MHz curvilinear ultrasound transducer to follow. Next, we defined the start point of the scanning trajectory by placing the transducer transversely at the lumbar region with the marked midpoint on the transducer footprint aligned with the scanning trajectory line, followed by slowly moving the transducer superiorly along the scanning trajectory until the 12th rib was clearly visible in the ultrasound image. While the transducer was at this position, a transverse line was drawn along the superior border of the transducer to demarcate the start point of each ultrasound scan. Similarly, the end point of the scanning trajectory was demarcated by drawing a transverse line along the inferior border of the transducer at the location where the anterior complex (ie, posterior longitudinal ligament and the vertebral body)[16] of the L5 at the L5-S1 interlaminar space could be clearly seen.

To evaluate the robustness and precision of the MRI-ultrasound registration technique on human participants, we scanned the lumbar region of each participant 5 times while he or she lay prone on a plinth with the abdomen supported by a pillow and kept at the same posture throughout the 5 ultrasound scans. During each scan, participants were instructed to hold their breath at the end of a normal exhalation for approximately 20 seconds while the ultrasound transducer was slowly swiped along the scanning trajectory line from the start to the end point, during which 600 transverse images were acquired at a frame rate of 30 Hz. A generous amount of ultrasound gel was applied on the lumbar region and the transducer footprint before each scan. This way, excellent acoustic coupling between the transducer and the skin surface could be achieved by swiping the transducer along the lumbar region with minimal pressure, yet without provoking vertebral segmental compression and joint motion. All ultrasound scans were acquired by a sonographer with more than 10 years of experience.

For each lumbar vertebra, a subset of ultrasound images that contained the target vertebra was extracted from the original 3D ultrasound dataset using ImageJ (National Institutes of Health, Bethesda, Maryland). To enhance the posterior bone surface of the vertebra, contrast stretching was applied to each ultrasound subset based on the overall stack histogram using the "enhance contrast" command within ImageJ with the percentage of saturated pixels set to 0.3%. Details of contrast stretching can be found elsewhere.[17] The processed ultrasound subsets were saved for later registration use. All image processing and analyses described earlier were performed by junior investigators independent of the ultrasound image acquisition.

MRI-Ultrasound Registration

For MRI-ultrasound registration of the lumbar vertebra, either feature-based or intensity-based algorithms can be used. The feature-based approaches rely on extracting bone surfaces from both ultrasound and MRI data and registering them using iterative closest point algorithms. A major challenge of feature-based registration is the difficulty of accurately extracting bone surfaces from ultrasound images. On the contrary, intensity-based registration techniques eliminate the need for segmenting bone surfaces from ultrasound data, which is the method of choice in this study. Given that the brightest pixels in ultrasound images are most likely caused by the reflection of ultrasound waves on the posterior vertebral surface, the 3D pose of each vertebra can be estimated from a set of 3 rotational (α, β, γ) and 3 translational (x, y, z) parameters that maximize the average pixel intensity of the ultrasound pixels that overlap with the MRI voxels of the posterior vertebral surface. Herein, α, β, and γ are the Z-Y-X Euler angles and x, y, and z relate the origin of the vertebral anatomical coordinate system regarding the laboratory coordinate system. Nonetheless, a challenge of intensity-based registration of human vertebra for in vivo application is that speckle noises and artifacts within the soft tissue are particularly detrimental at the vicinities on top of the transverse processes (TP), whereas some regions can even be brighter than bone surfaces in the B-mode ultrasound. We speculated that excluding the soft tissues surrounding the TP would improve the precision and robustness of the intensity-based registration. Given that it is challenging and time-consuming to separate the TP from surrounding soft tissues with confidence, we decided to test whether excluding both the TP and their surrounding soft tissues (denoted as TP complex) would improve the precision and robustness of the registration. This was accomplished by selecting a sub-volume of the 3D ultrasound dataset that included or excluded the TP complex, respectively, and

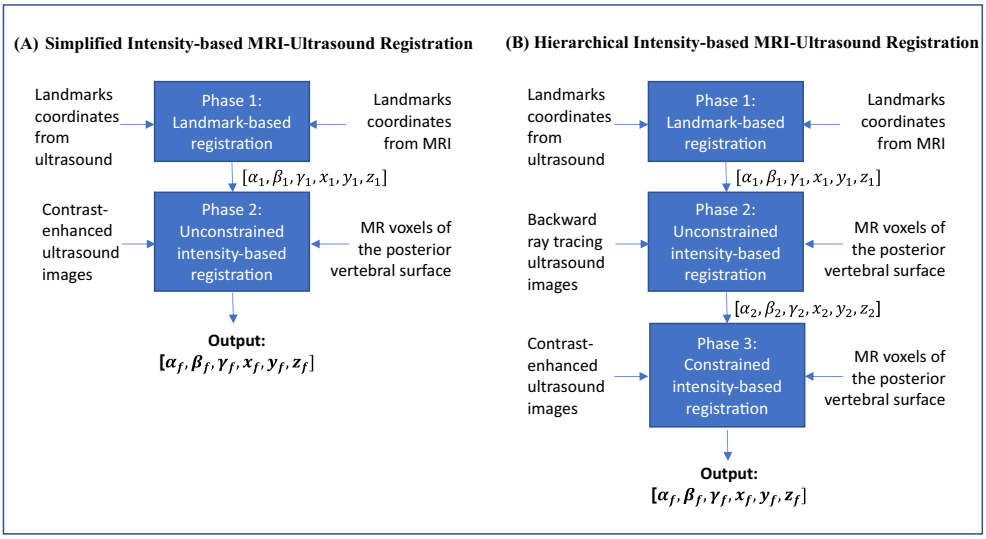

Figure 1. *Workflow of (A) the simplified and (B) the hierarchical intensity-based MRI-ultrasound registration algorithms.*

registering it with the corresponding MRI voxels of the posterior bone surface of the vertebra using either the simplified or hierarchical intensity-based MRI-ultrasound registration algorithms.

The workflows of the simplified and hierarchical intensity-based MRI-ultrasound registration algorithms are summarized in Figure 1. For both algorithms, the registration process began with providing an initial guess of the 3 rotational (α_1, β_1, γ_1) and 3 positional (x_1, y_1, z_1) parameters that were supposed to be closest to the true solution. This was achieved by digitizing 4 corresponding bony landmarks on both the ultrasound dataset and the MRI-reconstructed vertebral model and minimizing the average distance of the 4 point pairs using nonlinear optimization. We determined that the left and right superior and inferior articular processes could be located with confidence in both MRI model and ultrasound images, and hence these bony landmarks were selected manually in the current study. For the simplified intensity-based algorithm, an unconstrained intensity-based registration between the MRI voxels of the posterior vertebral surface and the contrast-enhanced ultrasound image subset of the target vertebra was implemented to obtain the final solution (α_f, β_f, γ_f, x_f, y_f, z_f). For the hierarchical intensity-based algorithm, a 2-step intensity-based registration process was implemented instead. First, a backward ray tracing technique[18] was applied to the contrast-enhanced ultrasound image subset to extract the ultrasound pixels in the vicinity of the posterior vertebral surface and registered with the MRI voxels of the posterior vertebral surface. This step aimed to minimize the detrimental effect of speckle noises and artifacts within the soft tissues on the registration solution. Next, the solution (α_2, β_2, γ_2, x_2, y_2, z_2) was further refined by constraining the search space within ± 8°/8 mm and re-registered with the contrast-enhanced ultrasound subset to get the final solution (α_f, β_f, γ_f, x_f, y_f, z_f). More details of the hierarchical registration algorithm can be found elsewhere.[13,14]

Data Analysis

In summary, a 3D pose of each lumbar vertebra (L1-L5) was determined by the 4 variants of the MRI-ultrasound registration (ie, simplified intensity-based registration [1] with and [2] without the TP complex, and hierarchical intensity-based registration [3] with and [4] without the TP complex). The relative spatial relationship between 2 adjacent vertebrae (L1-L2 and L4-L5) was also determined by calculating the anatomical joint angles and the x (right-left), y (anterior-posterior), and z (superior-inferior) components of the position vector of the origin of the anatomical frame of the superior vertebra regarding the anatomical frame of the inferior vertebra. Anatomical joint angles were defined as per Grood and Suntay,[19] where flexion or extension and axial rotation were to take place about the x-axis of the inferior vertebra and the z-axis of the superior vertebra, respectively, and lateral bending was about a floating axis, which was the vector product of the flexion or extension and axial rotation axes.

Given that it is unethical to implant fiducial markers in the lumbar vertebrae of healthy participants, a visualization tool developed in our previous study was used to provide qualitative assessment of the registration solutions.[14] This tool superimposed the registered MRI voxels of the posterior vertebral surface to the 3D ultrasound dataset as dark pixels (ie, zero intensity) and displayed the registered image slices as an image sequence. In this study, the quality of each registration was evaluated by the senior investigator

Table 1. *Comparison of Registration Performance Among the 4 MRI-Ultrasound Registration Variants*

Registration Variant	Successful Registration (%) [a]
Simplified with TP complex	91.7
Simplified without TP complex	100
Hierarchical with TP complex	91.7
Hierarchical without TP complex	100

MRI, magnetic resonance imaging; *TP*, transverse processes.

[a] The successfulness of each registration was qualitatively evaluated via the registered image sequence. Altogether, 120 registrations were evaluated from 24 vertebrae of the 5 healthy participants.

who was blinded to the registration conditions of the registered image sequences. Each registration was assigned as either successful or nonsuccessful. The percentage of successful registration among all registered lumbar vertebrae of the 5 participants was compared among the 4 MRI-ultrasound registration variants.

Precision at each degree of freedom (DOF) of each vertebra (ie, 3 Euler angles and 3 components of the position vector) and each motion segment (ie, 3 anatomical joint angles and 3 components of the position vector of the origin of the anatomical frame of the superior vertebra regarding the anatomical frame of the inferior vertebra) was determined by computing the standard deviation of each parameter among the 5 trials,[20,21] and the mean value of each parameter among the 5 participants at each vertebra (L1-L5) and at each motion segment (L1-L2 to L4-L5) were reported. The registration solutions among the 4 MRI-ultrasound registration variants were also compared with each other to check for their similarity. One-way repeated-measures analysis of variance (ANOVA) was performed to test the effect of registration approach on the precision of each rotational or translational parameter. For each registration approach, 1-way repeated-measures ANOVA was also performed to test whether there was any significant difference in precision among the 3 rotation parameters and among the 3 translational parameters, respectively. Post hoc comparisons were based on paired *t* tests with Bonferroni correction. The level of significance was set at .05 for all statistical tests.

Results

The MRI revealed that there was a spondylolysis at L5 (ie, lamina, spinous process, and inferior articular processes disconnected from the rest of vertebra) in 1 of the participants, and hence, that vertebra was excluded for registration evaluation. Altogether, 24 vertebrae from 5 healthy participants were evaluated, resulting in 120 registrations per MRI-ultrasound registration approach. Sample registered image sequences of successful registration (Video 1: L3 with TP complex; Video 2: L5 without TP complex) and nonsuccessful registration (Video 3: L1 with TP complex) are shown in the online version of the article as supplementary materials. Table 1 summarizes the registration performance of the 4 MRI-ultrasound registration approaches. It appears that the performance of both MRI-ultrasound registration algorithms (ie, simplified and hierarchical) are similar as judged by the quality of the registered image sequences. However, excluding the TP complex appears to further improve the percentage of successful registration (Table 1).

The difference of the registration solutions between registration approaches at each DOF of the tested vertebrae and motion segments is summarized in Tables 2 and 3, respectively. The data revealed that all of the difference values (except one equaled -1.59°) were in sub-degree and sub-millimeter levels, indicating the following: (1) excluding the TP complex should not affect the registration solutions, and (2) both simplified and hierarchical intensity-based MRI-ultrasound registration algorithms appeared to converge to the same solution.

Tables 4 and 5 summarize the precision of the 4 MRI-ultrasound registration approaches at each DOF of the tested vertebrae and motion segments, respectively. One-way repeated-measures ANOVA revealed that there was no significant difference in precision among the 4 MRI-ultrasound registration approaches ($P > .05$ at each DOF). However, when comparing the precision among the 3 rotational DOFs of the tested vertebrae, the precision of Euler angle α turned out to be significantly better than Euler angles β and γ, but there was no significant difference in precision between β and γ. This observation was noted no matter which MRI-ultrasound registration approaches were used. For the precision among the 3 translational DOFs of the tested vertebrae, a significant difference was only found in registration approaches that did not involve the TP complex. Specifically, post hoc comparison revealed that the precision of z translation was significantly better than those of x and y translation for the simplified MRI-ultrasound registration without the TP complex, and the precision of z translation was significantly better than the y translation only for the hierarchical MRI-ultrasound registration without the TP complex. For the tested motion segments, the precision of lateral bending was generally shown to be significantly poorer than axial rotation (all $P < .001$) and flexion or extension (3 paired comparisons reached the significant level). In addition, the precision of x translation (left–right translation) was generally shown to be significantly poorer than those of the y (anterior–posterior) (all $P < .015$) and z (superior–inferior) translations (2 paired comparisons reached the significant level).

The MR image processing (ie, segmentation, reconstruction, forward-ray tracing, landmark digitization) was a one-time process for each participant, which took about 1 hour/vertebra to accomplish. Ultrasound image processing (ie, extraction of a subset of ultrasound images for each

Table 2. *Difference (Mean [SD]) Between 3D Pose of Lumbar Vertebra Calculated by 4 Different MRI-Ultrasound Registration Variants*

	Difference (Mean [SD])			
Measurements	(1) - (3)	(2) - (4)	(1) - (2)	(3) - (4)
α (°)	0.33 (0.98)	-0.04 (0.72)	0.10 (1.14)	-0.04 (1.23)
β (°)	-0.60 (1.59)	0.29 (1.59)	0.44 (2.01)	1.00 (2.77)
γ (°)	0.19 (1.26)	0.45 (1.27)	0.05 (1.24)	0.14 (2.01)
x (mm)	-0.48 (0.91)	0.05 (0.50)	0.29 (1.17)	0.63 (1.26)
y (mm)	-0.08 (0.23)	-0.15 (0.26)	0.02 (0.68)	0.00 (0.53)
z (mm)	0.19 (0.89)	0.14 (0.99)	0.10 (0.88)	-0.08 (1.20)

(1) Simplified intensity-based registration without TP complex, (2) simplified intensity-based registration with TP complex, (3) hierarchical intensity-based registration without TP complex, and (4) hierarchical intensity-based registration with TP complex.
3D, 3-dimensional; *MRI*, magnetic resonance imaging; *SD*, standard deviation; *TP*, transverse processes.

Table 3. *Difference (Mean [SD]) Between 3D Pose of Motion Segment Calculated by 4 Different MRI-Ultrasound Registration Variants*

	Difference (Mean [SD])			
Measurements	(1) - (3)	(2) - (4)	(1) - (2)	(3) - (4)
Flexion/extension (°)	0.24 (1.55)	-0.48 (1.68)	0.42 (1.67)	-0.20 (2.56)
Lateral bending (°)	0.53 (1.76)	-0.51 (2.52)	-0.05 (2.47)	-1.59 (3.67)
Axial rotation (°)	0.38 (1.23)	-0.05 (0.81)	-0.10 (1.64)	-0.16 (1.65)
x (mm)	-0.26 (1.40)	0.04 (1.46)	-0.24 (2.52)	0.39 (2.31)
y (mm)	0.27 (0.91)	-0.06 (1.08)	0.37 (1.57)	0.01 (1.83)
z (mm)	-0.06 (1.07)	0.35 (1.18)	-0.11 (0.94)	0.23 (1.22)

(1) Simplified intensity-based registration without TP complex, (2) simplified intensity-based registration with TP complex, (3) hierarchical intensity-based registration without TP complex, and (4) hierarchical intensity-based registration with TP complex.
3D, 3-dimensional; *MRI*, magnetic resonance imaging; *SD*, standard deviation; *TP*, transverse processes.

vertebra, contrast enhancement, landmark digitization, back-ray tracing [hierarchical intensity-based registration only]) was a trial-specific task. On average, it took about 30 and 50 minutes, respectively, to prepare for the required ultrasound datasets of all 5 lumbar vertebrae for the simplified and hierarchical intensity-based registration use. In registration time, the simplified intensity-based registration algorithm took about 1 minute/vertebra to accomplish, whereas the hierarchical intensity-based registration algorithm took about 2 minutes/vertebra. Altogether, the total run time for each ultrasound trial was about 35 and 60 minutes, respectively, for the simplified and the hierarchical intensity-based registration algorithm. Hence, the simplified intensity-based registration can reduce the total run time by 42%.

Discussion

In our previous study, the nonionizing MRI-ultrasound registration approach was evaluated on 1 bone phantom (T12-L5) and 1 porcine cadaver (L2-L6).[13] Although these experiments confirmed the efficacy of the MRI-ultrasound registration approach under controlled conditions, they did not fully address its validity in vivo. In this study, we have extended our registration technique to live human participants to determine whether it can be used to quantify the 3D pose of lumbar vertebrae and motion segments in vivo. Our analysis and interpretation of data from 5 human participants also provided more statistical validity of our registration approach and allowed us to recognize its limitations. In addition, we have assessed the effectiveness of 4 variants of the MRI-ultrasound registration approach, including simplified and hierarchical registration with and without the TP included. Determining the algorithm that best registers the ultrasound images with the MRI model is important in that it promotes accuracy and efficiency if applied clinically.

As expected, our results showed that our MRI-ultrasound registration approach for in vivo measurements is promising but slightly inferior to our previous work with the porcine cadaver and bone phantom. For instance, the average

Table 4. *Precision (Mean ± SD) of the 4 MR-Ultrasound Registration Variants for the Quantification of the 3D Pose of Lumbar Vertebra*

Measurements	Simplified With TP Complex	Simplified Without TP Complex	Hierarchical With TP Complex	Hierarchical Without TP Complex
α (°)	0.78 ± 0.51	0.88 ± 0.43	0.93 ± 0.36	0.90 ± 0.52
β (°)	1.78 ± 0.99	1.67 ± 0.71	1.77 ± 0.95	1.89 ± 0.78
γ (°)	1.41 ± 0.74	1.26 ± 0.50	1.49 ± 0.80	1.33 ± 0.65
x (mm)	1.55 ± 1.68	1.27 ± 0.50	1.13 ± 0.65	1.27 ± 0.72
y (mm)	1.40 ± 0.80	1.38 ± 0.71	1.40 ± 0.81	1.50 ± 0.68
z (mm)	1.24 ± 0.47	0.94 ± 0.40	1.34 ± 0.81	1.00 ± 0.50

α, β, and γ are Euler angles in Z-Y-X rotation sequence that orientate the anatomical frame of a vertebra with respect to the laboratory frame. x, y, and z refer to the x, y, and z components of the position vector of the origin of the anatomical frame of a vertebra with respect to the laboratory frame. Reported values are the mean (SD) of the precision based on 24 vertebrae from 5 participants.
3D, 3-dimensional; *MR*, magnetic resonance; SD, standard deviation; *TP*, transverse processes.

Table 5. *Precision (Mean ± SD) of the 4 MR-Ultrasound Registration Variants for the Quantification of the 3D Pose of Lumbar Motion Segment*

Measurement	Simplified With TP Complex	Simplified Without TP Complex	Hierarchical With TP Complex	Hierarchical Without TP Complex
Flexion/extension (°)	1.45 ± 0.70	1.33 ± 0.75	1.85 ± 0.91	1.65 ± 0.95
Lateral bending (°)	2.42 ± 1.05	2.48 ± 1.28	2.21 ± 0.96	2.55 ± 0.74
Axial rotation (°)	1.16 ± 0.60	1.32 ± 0.47	1.04 ± 0.40	1.22 ± 0.58
x (mm)	2.39 ± 1.81	2.15 ± 0.98	2.10 ± 1.12	2.21 ± 0.78
y (mm)	1.04 ± 0.61	1.08 ± 0.50	1.49 ± 0.73	1.32 ± 0.80
z (mm)	1.27 ± 0.62	1.16 ± 0.38	1.50 ± 0.84	1.10 ± 0.49

Flexion or extension, lateral bending, and axial rotation are the anatomical joint angles per Grood and Suntay,[19] where flexion/extension and axial rotation were to take place about the x-axis of the inferior vertebra and the z-axis of the superior vertebra, respectively, and lateral bending was about a floating axis, which was the vector product of the flexion/extension and axial rotation axes. x, y, and z refer to the x, y, and z components of the position vector of the origin of the anatomical frame of the superior vertebra of a motion segment regarding the anatomical frame of the inferior vertebra. Reported values are mean (SD) of the precision based on 19 motion segments from 5 participants.
3D, 3-dimensional; *MR*, magnetic resonance; *SD*, standard deviation; *TP*, transverse processes.

precision of the simplified MRI-ultrasound registration approach without including TP was 1.71° and 1.46 mm, respectively, for intervertebral rotation and translation (cf. Koo and Kwok,[13] porcine cadaver: 1.26°/1.23 mm; dry bone phantom: 1.11°/0.86 mm). This finding can be partially explained by potential movements in the human participants. Unlike porcine cadaver and bone phantom, it is challenging for live human participants to keep their lumbar spine stationary for an extended period of time. In this study, we minimized posture changes between scanning trials by adopting a prone-lying protocol and providing special instructions to help participants to hold their breath at their functional residual capacity. Despite these efforts, differences in the point at which they held their breath could still occur, and likely yielded fluctuations in the 3D poses among scanning trials, especially that of the anteroposterior translation. Therefore, precision parameters reported in the current study depended not only on the registration error of the MRI-ultrasound registration approach, but also on the variation of the breath-holding point among scanning trials. We also noted that the precision of lateral bending and right–left translation were significantly inferior to the other DOFs, likely because the intensity-based objective function is less sensitive to these DOFs, and hence they should be interpreted with caution.

Our previous work on a porcine cadaver showed that the hierarchical algorithm was superior to the simplified intensity-based algorithm,[14] but results of the current study revealed that both registration algorithms appeared to have similar performance. This discrepancy was likely related to the difference in the way that the initial guess was estimated. An initial guess that is far from the true solution may result in the registration converging to a local maximum instead of the true solution. In our previous porcine cadaveric study, only 3 bony

landmarks (ie, the tips of spinous process and the left and right transverse processes) were used to estimate the initial guess. Given that uncertainty exists in interpreting these bony landmarks within the B-mode ultrasound, they may not be easily and consistently selected, which may make the initial guess far from the true solution. In this case, the hierarchical approach provided a means to confine the solution space closest to the true solution even when a relatively poor initial guess was used. In this study, 4 bony landmarks were selected instead, namely, the left and right inferior and superior articular processes. These landmarks were easily identifiable in the ultrasound scans because they exhibited bright and consistent reflections at each articulation. Given that more bony landmarks were used and that they could be selected with better confidence, we believed that this would substantially improve the chance to converge to the true solution. We noted that when registration failed using the 3 bony landmarks approach, the registration would be successful when using the articular processes as landmarks instead, further supporting the claim that the more numerous and easily identifiable landmarks are better for registering successfully, especially for more unclear scans.

Our results showed that excluding the TP and their surrounding soft tissues (ie, TP complex) did not affect the registration solution. Instead, it increased the likelihood of converging to the true solution. Although excluding the TP would reduce the area of available posterior vertebral surface for registration use, which might have a negative effect on the registration accuracy, our results implied that the spatial noise and artifacts in the surrounding soft tissues was a more critical factor that could affect the robustness of our MRI-ultrasound registration algorithm.

Given that the success of the MRI-ultrasound registration depends heavily on the quality of acquired ultrasound images,[22] to avoid the waste of time, effort, and money, it is imperative to check for ultrasound image quality before proceeding with any image processing work and MRI scan. In this study, a dated ultrasound scanner (Ultramark 400c, ATL Ultrasound Inc) was used. We anticipate that with technological advancement in ultrasound imaging[23,24] and processing methods, [25] the robustness and performance of the MRI-ultrasound registration will be further improved.

In the current study, we assumed that the brightest pixels in ultrasound images are most likely caused by the reflection of ultrasound waves on the posterior vertebral surface. Hence, the MRI-ultrasound registration was formulated as an optimization problem, where an intensity-based objective function that measured the average pixel intensity of the ultrasound pixels that overlapped with the MRI voxels of the posterior vertebral surface was maximized by determining a set of 3 rotational and 3 translational parameters using nonlinear optimization. Although this is highly plausible, maximizing the intensity-based objective function does not guarantee a successful registration, especially if the ultrasound data are noisy. In recent years, machine learning has been proposed for 3D image registration. For instance, Liao et al combined deep neural network and deep reinforcement learning to learn both a data-driven matching metric and a registration task-driven strategy simultaneously,[26] and hence it is supposed to minimize the detrimental effect of speckle noises and artifacts in 3D image registration. However, machine learning requires large amount of high-quality image data to train the models. Nonetheless, we believe that it is a highly promising approach for 3D image registration in the foreseeable future.

Although other 3D ultrasound techniques such as mechanical scanning[27] can provide a more precise and homogenous 3D ultrasound dataset for registration use, they lack flexibility in scanning mode. Our goal is to develop a radiation-free method to make in vivo 3D measurements of the human lumbar spine at different functional postures (eg, flexion, extension, lateral bending, and axial rotation) while participants stand, sit, or lie in a prone position. Therefore, the use of freehand scanning is justified because it is the only approach that can be implemented easily at different functional postures without any restriction. One may argue that freehand 3D ultrasound is a traditional technique for acquiring 3D ultrasound data, which may experience significant reconstruction errors, user-dependent imaging quality, and poor repeatability. The MRI-ultrasound registration technique reported in this study does not require 3D volume reconstruction of the 2D ultrasound images. All we need is to transform the local coordinates of each pixel from each ultrasound image to a common laboratory coordinate system based on the tracking information, and use these coordinate-transformed ultrasound pixels to register with the MRI voxels that correspond to the posterior surface of the vertebra. Hence, 3D volume reconstruction is irrelevant to our registration algorithm. In this study, we used a highly accurate optoelectronic measurement system to track the 3D poses of the ultrasound transducer and calibrated the system with a newly developed actuator-assisted approach to achieve a point reconstruction accuracy of 0.11 mm. We also developed a marking or scanning protocol to improve the scanning repeatability and facilitated the acquisition of high-quality axial ultrasound images throughout the lumbar region. Overall, we paid special consideration in our hardware selection, system calibration, and scanning protocol to minimize the potential drawbacks of freehand scanning on registration precision and accuracy.

Limitations

Although tremendous effort has been made to standardize the spinal configuration among repeated scans, as discussed earlier, the experimental protocol is inherently imperfect. This would potentially increase the variation of the registration solutions among trials and hence likely underestimated the precision of our MRI-ultrasound registration approach. Second, given that it would be unethical to place invasive

fiducial markers or bone pins in live human participants, we cannot directly quantify the accuracy of the registration solutions in the current study. Instead, we used the registered image sequence to qualitatively assess the registration solution because our previous studies have showed that if the registered image sequence makes sense, the solution was indeed comparable to the ground true solution.[13,14] In addition, given that the 4 registration algorithms led to similar solutions, it provided further support that the registration solutions are reasonable.

Conclusion

We successfully refined a MRI-ultrasound registration technique to make noninvasive, nonionizing 3D measurement of the lumbar spine segmental motion in vivo. Based on the comparison of the robustness and precision of 4 variants of the MRI-ultrasound registration technique on a cohort of human participants, we recommend the following: (1) using updated ultrasound technology to improve ultrasound image quality, (2) performing a preliminary check of ultrasound image quality to determine the applicability of the MRI-ultrasound registration technique in a participant-specific basis, (3) using the left and right superior and inferior acicular processes as bony landmarks to determine an initial guess, (4) adapting the simplified intensity-based algorithm with the TP complex excluded to streamline the registration process, and (5) collecting multiple trials to facilitate more comprehensive assessment. Given its nonionizing and noninvasive nature, the MRI-ultrasound registration approach is particularly well suited for repeated measurements and longitudinal follow-up in clinical settings.

Supplementary data to this article can be found online at https://doi.org/10.1016/j.jmpt.2019.03.008.

Practical Applications

- The MRI-ultrasound registration technique can be applied to live human participants to quantify the 3D pose of individual vertebra and motion segments.
- Its noninvasive and nonionizing nature make it particularly well suited for repeated measurements and longitudinal follow-ups.
- Excluding the TP and surrounding soft tissues in the registration process improves the success rate of the registration.
- A simplified intensity-based algorithm is recommended, because it can streamline the registration process without compromising the precision.

Acknowledgment

The authors thank Drs. Mary Balliett and Madison Nash for their help in participant screening. We also thank Amy Lin and Preya Patel for their assistance in image and data processing.

Funding Sources and Conflicts of Interest

This work was supported by a pilot grant of University of Rochester Center for Advanced Brain Imaging & Neurophysiology. Robert L. Crews was supported by a summer internship program of New York Chiropractic College. No conflicts of interest were reported for this study.

Contributorship Information

Concept development (provided idea for the research): T.K.K., W.E.K.
Design (planned the methods to generate the results): T.K.K.
Supervision (provided oversight, responsible for organization and implementation, writing of the manuscript): T.K.K.
Data collection/processing (responsible for experiments, patient management, organization, or reporting data): T.K.K., R.L.C., W.E.K.
Analysis/interpretation (responsible for statistical analysis, evaluation, and presentation of the results): T.K.K., R.L.C.
Literature search (performed the literature search): T.K.K.
Writing (responsible for writing a substantive part of the manuscript): T.K.K., R.L.C.
Critical review (revised manuscript for intellectual content, this does not relate to spelling and grammar checking): W.E.K.

References

1. Esola MA, McClure PW, Fitzgerald GK, Siegler S. Analysis of lumbar spine and hip motion during forward bending in subjects with and without a history of low back pain. *Spine (Phila Pa 1976).* 1996;21(1):71-78.
2. McClure PW, Esola M, Schreier R, Siegler S. Kinematic analysis of lumbar and hip motion while rising from a forward, flexed position in patients with and without a history of low back pain. *Spine (Phila Pa 1976).* 1997;22(5):552-558.
3. Passias PG, Wang S, Kozanek M, et al. Segmental lumbar rotation in patients with discogenic low back pain during functional weight-bearing activities. *J Bone Joint Surg Am.* 2011;93(1):29-37.
4. Cramer GD, Henderson CN, Little JW, Daley C, Grieve TJ. Zygapophyseal joint adhesions after induced hypomobility. *J Manipulative Physiol Ther.* 2010;33(7):508-518.
5. Koo TK, Guo JY, Ippolito C, Bedle JC. Assessment of scoliotic deformity using spinous processes: comparison of different analysis methods of an ultrasonographic system. *J Manipulative Physiol Ther.* 2014;37(9):667-677.
6. Gracovetsky S, Newman N, Pawlowsky M, Lanzo V, Davey B. Robinson L. A database for estimating normal spinal motion

derived from noninvasive measurements. *Spine (Phila Pa 1976).* 1995;20(9):1036-1046.
7. Dickey JP, Pierrynowski MR, Bednar DA, Yang SX. Relationship between pain and vertebral motion in chronic low-back pain subjects. *Clin Biomech (Bristol, Avon).* 2002;17(5):345-352.
8. Aiyangar AK, Zheng L, Tashman S, Anderst WJ, Zhang X. Capturing three-dimensional in vivo lumbar intervertebral joint kinematics using dynamic stereo-X-ray imaging. *J Biomech Eng.* 2014;136(1):011004.
9. Pearcy MJ. Stereo radiography of lumbar spine motion. *Acta Orthop Scand Suppl.* 1985;212:1-45.
10. Li G, Wang S, Passias P, Xia Q, Li G, Wood K. Segmental in vivo vertebral motion during functional human lumbar spine activities. *Eur Spine J.* 2009;18(7):1013-1021.
11. Ochia RS, Inoue N, Takatori R, Andersson GB, An HS. In vivo measurements of lumbar segmental motion during axial rotation in asymptomatic and chronic low back pain male subjects. *Spine (Phila Pa 1976).* 2007;32(13):1394-1399.
12. Kulig K, Powers CM, Landel RF, et al. Segmental lumbar mobility in individuals with low back pain: in vivo assessment during manual and self-imposed motion using dynamic MRI. *BMC Musculoskelet Disord.* 2007;8:8.
13. Koo TK, Kwok WE. A non-ionizing technique for three-dimensional measurement of the lumbar spine. *J Biomech.* 2016;49(16):4073-4079.
14. Koo TK, Kwok WE. Hierarchical CT to ultrasound Registration of the lumbar spine: a comparison with other registration methods. *Ann Biomed Eng.* 2016;44(10):2887-2900.
15. Koo TK, Silvia N. Actuator-assisted calibration of freehand 3D ultrasound system. *J Healthc Eng.* 2018;2018:9314626.
16. Balki M, Lee Y, Halpern S, Carvalho JC. Ultrasound imaging of the lumbar spine in the transverse plane: the correlation between estimated and actual depth to the epidural space in obese patients. *Anesth Analg.* 2009;108(6):1876-1881.
17. Fisher R, Perkins S, Walker A, Wolfart E. Contrast stretching. Available at: http://homepages.inf.ed.ac.uk/rbf/HIPR2/stretch.htm#1 Accessed March 4, 2019.
18. Yan CX, Goulet B, Pelletier J, Chen SJ, Tampieri D, Collins DL. Towards accurate, robust and practical ultrasound-CT registration of vertebrae for image-guided spine surgery. *Int J Comput Assist Radiol Surg.* 2011;6(4):523-537.
19. Grood ES, Suntay WJ. A joint coordinate system for the clinical description of three-dimensional motions: application to the knee. *J Biomech Eng.* 1983;105(2):136-144.
20. Haque MA, Anderst W, Tashman S, Marai GE. Hierarchical model-based tracking of cervical vertebrae from dynamic biplane radiographs. *Med Eng Phys.* 2013;35(7):994-1004.
21. Anderst WJ, Baillargeon E, Donaldson WFIII, Lee JY, Kang JD. Validation of a noninvasive technique to precisely measure in vivo three-dimensional cervical spine movement. *Spine (Phila Pa 1976).* 2011;36(6):E393-E400.
22. Winter S, Pechlivanis I, Dekomien C, Igel C, Schmieder K. Toward registration of 3D ultrasound and CT images of the spine in clinical praxis: design and evaluation of a data acquisition protocol. *Ultrasound Med Biol.* 2009;35(11):1773-1782.
23. Huang Q, Wu B, Lan J, Li X. Fully automatic three-dimensional ultrasound imaging based on conventional B-scan. *IEEE Trans Biomed Circuits Syst.* 2018;12(2):426-436.
24. Huang Q, Zeng Z, Li X. 2.5-D extended field-of-view ultrasound. *IEEE Trans Med Imaging.* 2018;37(4):851-859.
25. Zhuang B, Rohling R, Abolmaesumi P. Accumulated angle factor-based beamforming to improve the visualization of spinal structures in ultrasound images. *IEEE Trans Ultrason Ferroelectr Freq Control.* 2018;65(2):210-222.
26. Liao R, Miao S, de Tournemire P, et al. An artificial agent for robust image registration. *Proc Conf AAAI Artif Intell.* 2017 Feb:4168-4175.
27. Huang Q, Yang Z, Hu W, Jin LW, Wei G, Li X. Linear tracking for 3D medical ultrasound imaging. *IEEE Trans Cybern.* 2013;43(6):1747-1754.